

Types of bathymetry data from Gebco

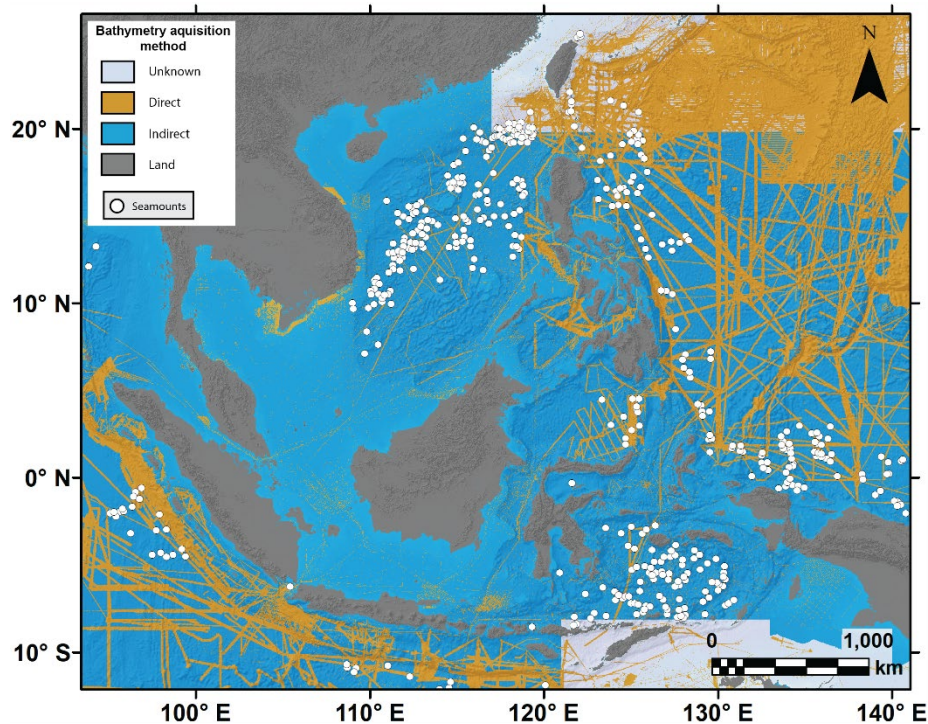


Fig. S1. Gebco 2021 bathymetry map showing areas where bathymetry was acquired through direct (e.g. echo-sounding from boats) and indirect (e.g. grid point interpolations) methods.

Linking seamount morphology and evolution stage with their potential hazards

Seamount morphotype

Simple cones

Simple cones are regularly-shaped conical edifices with only one vent. This morphotype indicates a relatively simple volcanic history. It can be either short-lived (i.e. one single eruptive event that formed a relatively small and regularly-shaped cone, or clusters of simple cones) or characterised by more or less consistent volcanic activity through time from a central vent, with no lateral migration of the magma source. By using subaerial volcanic morphologies as a comparison, we can assume that simple cones are mostly monogenetic (short-lived), and they usually reflect simple shallow plumbing systems, both for isolated cones and clusters of cones (Valentine et al., 2017). This is particularly common in areas of distributed volcanism (Connor et al., 2012; Gallant et al., 2018; Verolino et al., 2022), where magma rises through the shallow substrate through preferential pathways, either controlled by tectonics (Connor et al., 2000), by eruptive timeframes (Pansino et al., 2019), or by variable thermal conditions (Cole et al., 2023). However, the link between simple cones formed in subaerial environments and those formed underwater is not straightforward, given the broad lack of information (e.g. seismic data to detect major faulting systems in the substrate), and enhanced complexity for the presence of wet and loose sediments in subaqueous settings (Schipper et al., 2011).

Simple cones can be of different size, however, those formed in shallow waters are generally smaller than those formed at large water depths, this is because of the lack of accommodation space. For example, on continental shelves, once the seamount emerges, it experiences important erosional processes that control its height, while in deep-sea environment there is negligible erosion associated with water, and the seamount has enough space to keep growing vertically through the water column (Staudigel and Koppers, 2015). Obviously, the main controlling factor is the continued volcanic activity and associated eruptive style.

Composite edifices

This category includes irregularly shaped multi-vent edifices, volcanic ridges, and cones formed on flanks of larger edifices. Their morphology reflects the complexity of the plumbing system (e.g. shallow dike intrusions, shallow lateral migration of magma, formation of fissures), abundant magma supply, and/or variation in eruptive style (which plays a role in the distribution of the deposits). The morphological convolution of this morphotype can also derive from the presence of surface structures associated with the seamount flank instabilities (e.g. horseshoe-like debris avalanche amphitheatres). The occurrence of more than one vent, the relatively high probability of flank collapse, and the large areal distribution of the deposits makes this morphotype more hazardous than simple cones. There are several examples worldwide of well-documented erupting composite seamounts, particularly in shallow waters, one of them is the Sarigan seamount, northern Mariana Islands. This seamount erupted in 2010 from a depth of ~200 m, producing an eruptive column that breached the water surface and reached 12 km in the atmosphere, and pyroclastic deposits up to 50 m thick on the surrounding seafloor (Embley et al., 2014). This eruption was considered of moderate to high intensity (VEI= 3-4), but luckily occurred in a rather remote area of the Pacific Ocean and no damage was recorded. Recorded cases from deep waters composite edifices also exist, for example the submarine volcano Fani Maoré near Mayotte island (3,500 m b.s.l.), which produced the largest effusive eruption ever recorded after Laki (Iceland, 1783 CE) (Berthod et al., 2021). This volcano is part of a seamounts chain, extending WNW-ESE, between Madagascar and eastern Mozambique, Africa, and has been discovered thanks to intense seismic activity taking place in the period 2018-2021, and subsequent oceanographic campaigns that provided a wealth of data (Berthod et al., 2023).

Caldera

Calderas are volcanic edifices characterised by a central prominent depression. Despite there are different types of calderas (e.g. piston-like, funnel-like, trapdoor), a common formation mechanism is the more or less rapid magma withdrawal from a shallow magma chamber. There is no definition of calderas based on their minimum diameter, however, according to the Collapse Caldera Database –

CCDB (Sobradelo et al., 2010), which includes both subaerial and some subaqueous calderas, about 50% of them have diameter < 10 km, which is consistent with what we have classified here as a caldera (4 - 8 km diameter). Note that this range of diameters is utilised as a guideline in this study. We acknowledge, however, that submarine calderas outside of this range, particularly those < 4 km, may also exist in the region, but their identification may be challenging due to relatively low resolution. In subaerial environments, caldera are mostly associated with high-magnitude explosive activity, therefore we can assume the same for most submarine calderas, particularly those at water depths < 1,000 m, subject to a relatively lower hydrostatic pressure (Cas, 1992). Most of the known and studied submarine calderas on Earth are found along volcanic arcs and are within 1000 m water depth. They have a rather regular shape with a sub-circular central depression (e.g. Havre caldera, Hunga caldera, Krakatau caldera; ~ 4 - 8 km diameter). A few submarine calderas, instead, have more complex shapes, and are deeper than 2000 m. One example is the Axial caldera, on the Juan de Fuca Ridge, which has its summit at about 1,300 m b.s.l. and its caldera floor at about 1,800 m b.s.l. in its deeper part. The caldera is 3x8 km wide, with an unusual elongated horseshoe-like shape, and its formation has been attributed to rapid withdrawal of magma from a shallow reservoir through eruption of voluminous lava flows, similarly to Kilauea, Hawaii (Clague et al., 2019). However, another recent work attributed the Axial caldera formation to a cataclysmic phreatomagmatic explosive eruption, from the study of the deposits (Danielsen, 2019). This highlights the fact that controversy still exists about these complex submarine systems, even when they are well studied and monitored.

Guyot

Guyots are seamounts with a flat summit and relatively steep flanks, which result from wave erosion once they emerge above sea level and then stop erupting, subsequently sinking below sea level for thermal subsidence and/or plate movement towards the subduction zone. They are considered the least hazardous among the morphotypes investigated here, because of their expected long period of inactivity. However, they can still represent a threat in two ways: 1) Their flanks can be subject to collapses in case of nearby seismic activity; and 2) They may represent invisible obstacles for submersibles if not charted. Additionally, some guyots may experience renovated volcanic activity, with formation of secondary cones on its summit or on their flanks (Mel'nikov et al., 2016).

Seamount growth stage

Based on the growth stages proposed by Staudigel and Clague (2010) (Table 2 – main manuscript), seamounts may go through all growth stages or just some of them, depending on the initial formation environment (water depth) and tectonic setting. Seamounts that initially formed in deep waters can potentially evolve from stage 1 to 5, growing from deep (stages 1 and 2) to shallow waters (stage 3) through both explosive and effusive activity, eventually emerge (stage 4), and when the activity ceases

their summits go through important erosional processes, with the seamount “sinking” as a result of subsidence and/or plate movement towards subduction zones (stage 5). Some seamounts may stop to stage 1, 2 or 3, depending on magma supply. Also, stage 3 seamounts may “downgrade” to stage 2 if volcanic activity stops for a relatively long time and they move towards subduction zones. However, once stage 3 seamounts reach stage 4, they will likely evolve through time to stage 5, given the dominance of destructive (erosion) versus constructive (eruption) processes. Stage 5 seamounts can be found both in shallow- and deep-water environments, and this gives an indication about the relative timing between emersion and erosion/subsidence (deep stage 5 seamounts are older than shallow ones), hence providing insights about relative plate movements. Some seamounts, however, never go through stage 1 and 2 if formed in shallow waters (e.g. on continental shelves). They start from stage 3 (water depths < 700 m) and either stop there or emerge forming short- or long-lived islands, based on the type of volcanic activity (explosive ± effusive). Below we provide a background on all growth stages in function on their potential hazards, with associated examples, where available.

Stage 1 and stage 2 seamounts

Overall, these types of seamounts are rarely investigated in terms of hazard potential as they are located in deep waters; however, although low, they still present some element of hazard through lava flows and debris avalanches, and less likely but not negligibly, also through pyroclastic density currents (PDCs) and pumice rafts. Seamounts at these stages can experience landslides (Harders et al., 2014), and eventually damage nearby submarine infrastructures. Even though there is no recorded case of cable damage from stage 1 or stage 2 seamounts, they should be considered when planning cables installation at large water depths in proximity of seamounts. Associated to landslides there is the tsunami hazard. Volcanic tsunamis can be formed through various mechanisms (Paris et al., 2014), however, those expected for stage 1 and stage 2 volcanoes are landslide-tsunamis. One example is proposed by Omira et al. (2016), who investigated the Hirondeille Seamount, NE Atlantic, as a potential source of landslide-generated tsunamis. In particular, Omira et al. describe a landslide on the south flank of the seamount at a depth > 3,000 m b.s.l., with approximate volume of ~500 km³, which likely produced a mega-tsunami that affected the coasts of Iberia and Morocco. Therefore, even if stage 1 and stage 2 seamounts are little represented in historical landslide/tsunami databases (e.g. NCEI/WDS), the Hirondeille seamount shows us what they are capable of, particularly stage 2 seamounts. Similarly to debris avalanches, submarine lava flows can damage submarine infrastructures as well. Generally, underwater lava flows are thought to cover small distances from the vent because of their immediate cooling at the contact with water, however, there are natural examples, also supported by numerical modelling, where deep lava flows (> 1,500 m b.s.l.) have runouts of over 100 km (Gregg and Fornari, 1998), this is relevant for impact assessments from deep-

sea volcanic eruptions. PDCs and eruption columns have been widely observed subaerially or at the land/water interface, and rarely observed in shallow waters (e.g. NW Rota-1; Deardorff et al., 2011). Although there is no direct observation of such phenomena in deep-sea environments, they have been inferred through the study of the deposits (Murch et al., 2019) and analogue experiments (Newland et al., 2022). Damage to submarine infrastructure from such phenomena has never been reported to our knowledge, however, the consequences are potentially similar to those produced by submarine landslides. Pumice rafts are another possible hazard from these seamounts, particularly from stage 2. An example is represented by Havre seamount, in the Kermadec Arc, which erupted in 2012 from a depth of about 1000 m, and was considered one of the largest historic silicic submarine volcanic eruptions in recent times (Carey et al., 2014). It produced a large pumice raft, among other hazards, which drifted away for thousands of kilometers and covered a total area of more than 500,000 km² (Jutzeler et al., 2014), about the size of Thailand. Luckily, it did not affect ship traffic in a significant way, also given the remote location of the eruption. Lastly, even non-erupting stage 1 and stage 2 seamounts may represent a hazard themselves as obstacles for submersibles when not charted. For example, on 2nd October 2021, a USA nuclear submarine collided against a seamount in the South China Sea, injuring 11 crew members (the exact location of the seamount was not released by the competent authorities – source: CNN. This incident reminds us that the scarcity and low quality of bathymetric data in some regions results in a number of uncharted seamounts, and this is a major issue in areas such as SEA, where military operations with submersibles are common.

Stage 3 and stage 4 seamounts

These categories are the most studied and potentially the most hazardous ones across all stages, particularly stage 4 seamounts. However, an advantage in studying stage 4 seamounts, is that they are visible above sea level and easier to access and investigate. Most of stage 3 and stage 4 seamounts are characterised by Surtseyan volcanic activity (i.e. emergent or nearly emergent volcanoes, resulting from explosive interaction between rising magma and external water). There are many examples worldwide from all tectonic settings, but the most complete one is Surtsey volcano, Iceland (1963-1967). This eruption formed the main island of Surtsey through initial subaqueous and then mixed subaqueous/subaerial explosive activity, and later subaerial effusive one. Other examples are from the eastern continental shelf of southern New Zealand (Moorhouse et al., 2015; Scott et al., 2020), Azores Islands in the North Atlantic (Cole et al., 2001), and Jeju Island, about 70 km offshore south of South Korea (Murtagh et al., 2011). Similarly, there are also examples from lacustrine environments from the western USA (Pahvant Butte and Black Point; Verolino et al., 2018, 2019), Philippines (Taal; Waters and Fisher, 1971) and Vanuatu (Ambae Island; Németh et al., 2006), with the processes and products being equivalent to those occurring in shallow marine waters. Surtseyan activity is

responsible for the formation of a wide spectrum of hazards that are common both in subaqueous and subaerial environments, including PDCs, eruptive columns, delivery of large clasts, formation of harmful very fine ash, sector collapses and tsunamis. All these hazards from stage 3 and stage 4 seamounts can expose people and infrastructures (marine and terrestrial), besides disrupting air and ship traffic. One sad example is represented by the destruction of the Japanese vessel Kaiyo Maru No 5 during a shallow submarine eruption off the coasts of Japan in 1952; according to Dietz and Sheehy (Dietz and Sheehy, 1954), the vessel was destroyed because of an intense and unexpected submarine volcanic explosion and associated tsunami. The Hunga volcano eruption on January 15th, 2022, produced near-field and far-field tsunamis through different mechanisms, including those produced by submarine explosions (Pakoksung et al., 2022) and meteorological-tsunamis, with run-ups of up to 15 m. The impact was significant, both for the Tongan population and also for coastal communities in Japan, central America and south America. Pumice rafts are also a possible hazard from stage 3 and stage 4 seamounts. A recent example is from the 2021 Fukutoku-Oka-no-Ba eruption, in Japan. Fukutoku-Oka-no-Ba volcano was a stage 3 seamount evolving to stage 4 during the eruption, which produced a large amount of pumice that drifted about 1,300 km west of the volcano in about 2 months. The pumice raft was stranded along the northern coasts of Okinawa Island and had a huge local ecological impact, besides largely affecting fishing boats (Ohno et al., 2022). This was one of the first ever documented cases of impact from pumice rafts.

Stage 5 seamounts

They are equivalent to guyots by definition (see previous section on morphotypes), and represent the last evolution stage of seamounts. As mentioned earlier they are used to study relative plate movements, for examples providing insights about absolute plate motions (Wessel and Kroenke, 1997).

Supplementary 'potential exposure' results

In addition to the aggregated exposure results shown in Fig. 5 (main manuscript), here we report averaged values for the assets considered across the five EEZs with exposure > 0 (Figs. S2). National exposure potential differs for the different growth stages and exposure categories. In general, exposure to the most hazardous stage of seamount (Stage 4) dominates the exposure potential assessment, with Taiwan the most exposed to this seamount stage, and Indonesia and Philippines second for population and cable length/ship traffic, respectively. We discuss trends for exposure to each growth stage in the below, from most hazardous to least:

- Stage 4, stage 3 and stage 2: Andaman and Nicobar Islands (India) only includes two seamounts (both stage 4), which expose an average of about 5k people and have moderate exposure to ship traffic (2.86×10^{10} AIS/hour); submarine cables are not found within the 100 km radius of these seamounts.

Indonesia presents high level of exposure for population (122 seamounts with exposure > 0), particularly for stage 4, 3 and 2 seamounts (~ 100 – 600k people); moderate to low exposure for submarine cables (16 seamounts with > 0 km of cables exposed) with seamounts from only stage 4 and stage 3 categories, and an average of about 300 km of cables exposed for each growth stage. Ship traffic exposure around Indonesia is the lowest among all countries considered (2.94×10^{10} – 4.48×10^{10} AIS/hour). The Philippines has between around 20k (stage 4) and 85k (stage 3) people/seamount (9 seamounts with population exposure > 0) exposed, between about 700 and 1400 km of cables/seamount (73 seamounts exposing > 0 km of cables, of which 1165 km for stage 4 seamounts), and 5.95×10^{10} – 1.19×10^{11} AIS/hour for ship traffic (stage 4 seamounts have an average of 8.86×10^{10} AIS/hour, from 95 seamounts in total), which is among the highest in the region. Taiwan is represented by only stage 3 and stage 4 seamounts for population exposure (n= 6), which is the highest in the region (average of 3.3M for stage 3 and 5M for stage 4 seamounts); also cables and ship traffic exposure are the highest, with an average of over 2000 km of cables (from 43 seamounts), and 5.6×10^{11} AIS/hour for boat traffic (43 seamounts), both for stage 4 seamounts, but also the other growth stages are represented here. Vietnam, with the majority of the seamounts being stage 2 (n= 22) and stage 3 (n= 22), expose an average of nearly 20,000 people (for stage 3 seamounts); cables exposure is around 1000 km for all categories (except stage 5 seamounts, not represented here); and ship traffic is between 3.24×10^{10} (stage 4) and 5.76×10^{10} AIS/hour (stage 3). Finally, the overlapping claim waters include 48 seamounts in total (stage 1 n=3; stage 2 n= 34, stage 3 n= 11), of these, 3 seamounts expose population, while 48 seamounts expose population and ship traffic. Population exposure is among the lowest in this region, with averages of 368 people for stage 2 seamounts and 15 people for stage 3. Submarine communication cables exposure has an average of nearly 600 km from each category (from stages 2 and 3). Lastly, ship traffic is around 3.8×10^{10} AIS/hour.

- Stage 1 and stage 5: exposure associated with these seamounts is to be considered low, given their rather low hazard potential. Philippines appears as the country with higher exposure to low hazard seamounts (particularly stage 5 seamounts), for all assets. Indonesia presents high population exposure from both stage 1 and stage 5 seamounts, and moderate to low exposure in terms of ship traffic density ($> 2.0 \times 10^{10}$ AIS/hour); no stage 1 or stage 5 seamount exposes submarine communication cables in Indonesian waters. Taiwan exposes submarine cables and ship traffic (only from stage 1 seamounts), with > 1200 km of cables and $\sim 5 \times 10^{10}$ AIS/hour respectively; population exposure to both stage 1 and stage 5 seamounts is zero. Vietnam has relatively high exposure for cables (> 1000 km – stage 1) and ship traffic ($\sim 5 \times 10^{10}$ AIS/hour – stage 1), and rather low exposure for population (20 people – stage 1). Lastly, the overlapping claim waters have only stage 1 seamounts exposing submarine cables (~ 580 km) and ship traffic ($< 5 \times 10^{10}$ AIS/hour).

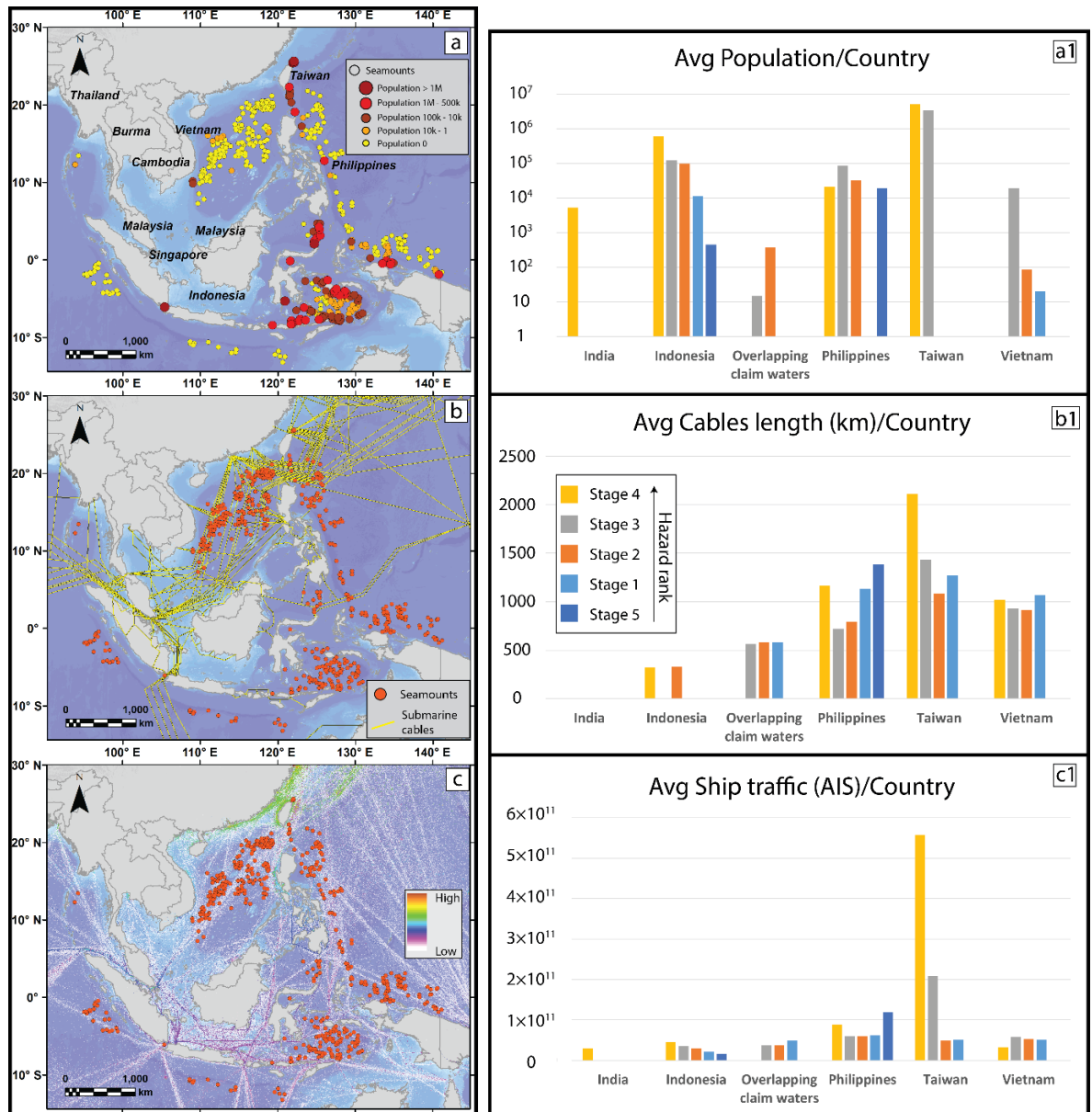


Figure S2. Exposure maps of the study region for population (a), submarine communication cables (b) and ship traffic density (c), and associated averaged exposure by country (a1 to c1). Note that exposure was considered only for seamounts with exposure higher than zero. Growth stages are ordered by hazard potential (see also Table 3 – Methods – main manuscript). For the EEZs refer to Fig. 3 (main manuscript).

Hazard weighted density map of seamounts

We ran a sensitivity test of the hazard weighted seamount density assessment by only including stage 3 and stage 4 seamounts (Fig. S3), weighted 0.4 and 0.6 respectively. This map shows negligible differences compared to that produced by including all seamount stages (Fig. 6). Minor differences of low seamounts density are reported in the Halmahera Sea and in the portion of Pacific Ocean to the northeast of northern Philippines, not appearing in this map.

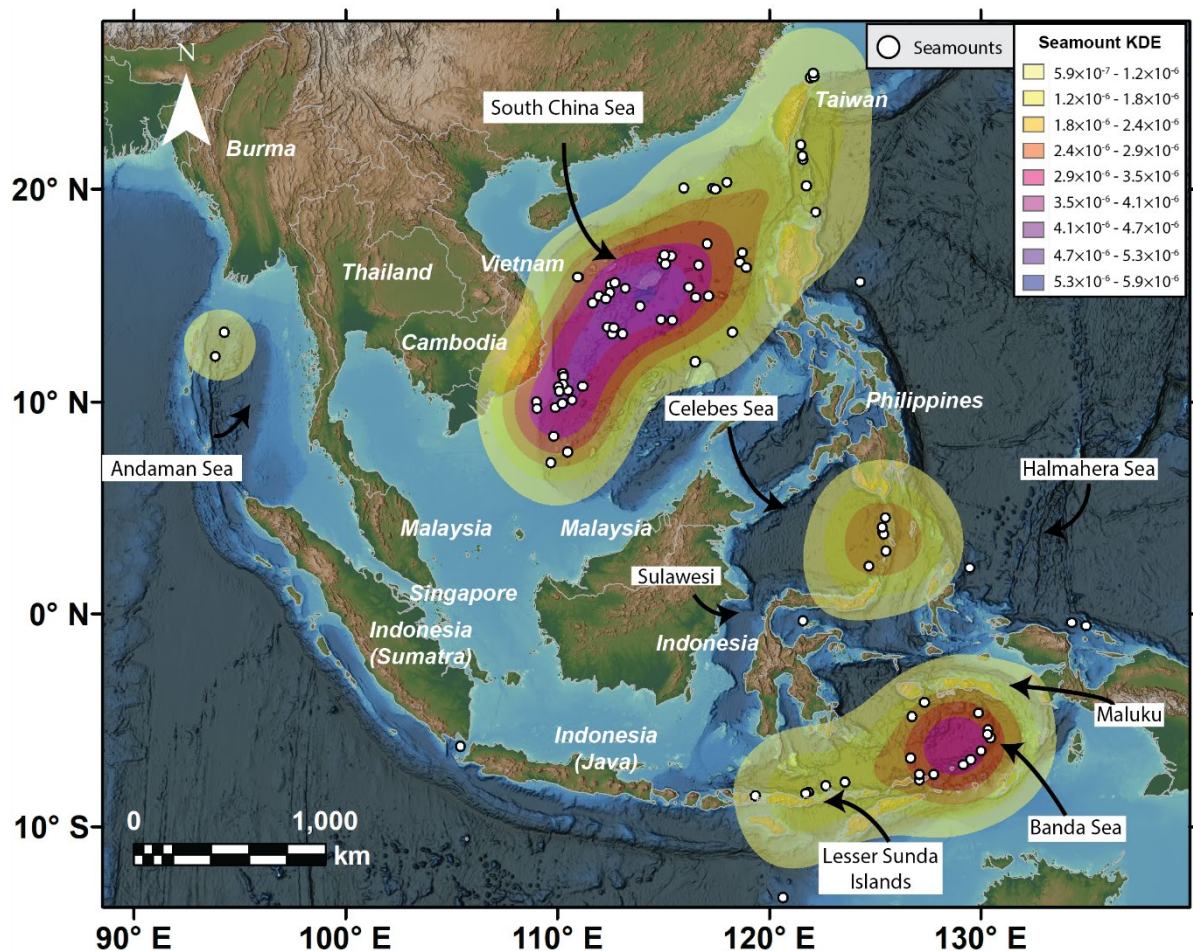


Figure S3. Kernel density map of seamounts in the region of interest weighted by their growth stage, hence hazard potential. Note that only stage 3 and stage 4 seamounts were used to produce this map.

Supplementary References

Berthod, C., Médard, E., Bachèlery, P., Gurioli, L., Di Muro, A., Peltier, A., Komorowski, J.-C., Benbakkar, M., Devidal, J.-L., Langlade, J., Besson, P., Boudon, G., Rose-Koga, E., Deplus, C., Le Friant, A., Bickert, M., Nowak, S., Thion, I., Burckel, P., Hidalgo, S., Kaliwoda, M., Jorry, S. J., Fouquet, Y., and Feuillet, N.: The 2018-ongoing Mayotte submarine eruption: Magma migration imaged by petrological monitoring, *Earth and Planetary Science Letters*, 571, 117085, <https://doi.org/10.1016/j.epsl.2021.117085>, 2021.

Berthod, C., Komorowski, J.-C., Gurioli, L., Médard, E., Bachèlery, P., Besson, P., Verdurme, P., Chevrel, O., Di Muro, A., Peltier, A., Devidal, J.-L., Nowak, S., Thion, I., Burckel, P., Hidalgo, S., Deplus, C., Loubrieu, B., Pierre, D., Bermell, S., Pitel-Roudaut, M., Réaud, Y., Fouchard, S., Bickert, M., Le Friant, A., Paquet, F., Feuillet, N., Jorry, S. L., Fouquet, Y., Rinnert, E., Cathalot, C., and Lebas, E.: Temporal magmatic evolution of the Fani Maoré submarine eruption 50 km east of Mayotte revealed by in situ sampling and petrological monitoring, *Comptes Rendus. Géoscience*, 354, 195–223, <https://doi.org/10.5802/crgeos.155>, 2023.

Carey, R. J., Wysoczanski, R., Wunderman, R., and Jutzeler, M.: Discovery of the Largest Historic Silicic Submarine Eruption, *Eos, Transactions American Geophysical Union*, 95, 157–159, <https://doi.org/10.1002/2014EO190001>, 2014.

Cas, R. A. F.: Submarine volcanism; eruption styles, products, and relevance to understanding the host-rock successions to volcanic-hosted massive sulfide deposits, *Economic Geology*, 87, 511–541, <https://doi.org/10.2113/gsecongeo.87.3.511>, 1992.

Clague, D. A., Portner, R. A., Paduan, J. B., Le Saout, M., and Dreyer, B. M.: Formation of the summit caldera at Axial Seamount. In *AGU Fall Meeting Abstracts (Vol. 2019, pp. V43C-0217)*, 2019.

- CNN: Navy investigation finds submarine crash in South China Sea was 'preventable'. Mon May 23, 2022. <https://edition.cnn.com/2022/05/23/politics/uss-connecticut-investigation/index.html#:~:text=Navy%20investigation%20finds%20submarine%20crash%20in%20South%20China%20Sea%20was%20preventable%20,-By%20Oren%20Liebermann&text=A%20Navy%20investigation%20into%20the,as%20well%20as%20other%20errors.,n.d.>
- Cole, P. D., Guest, J. E., Duncan, A. M., and Pacheco, J.-M.: Capelinhos 1957–1958, Faial, Azores: deposits formed by an emergent surtseyan eruption, *Bull Volcanol*, 63, 204–220, <https://doi.org/10.1007/s004450100136>, 2001.
- Cole, R. P., White, J. D. L., Baxter, R. J. M., Bowman, M. H., Dürig, T., Fleming, M., Pooley, B., Farra Engineering Ltd, Ruz-Ginouves, J., Gudmundsson, M. T., Cronin, S. J., Leonard, G. S., and Valentine, G. A.: A model volcanic fissure with adjustable geometry and wall temperature, *Bull Volcanol*, 85, 15, <https://doi.org/10.1007/s00445-023-01627-2>, 2023.
- Connor, C. B., Stamatakis, J. A., Ferrill, D. A., Hill, B. E., Ofoegbu, G. I., Conway, F. M., Sagar, B., and Trapp, J.: Geologic factors controlling patterns of small-volume basaltic volcanism: Application to a volcanic hazards assessment at Yucca Mountain, Nevada, *J. Geophys. Res.*, 105, 417–432, <https://doi.org/10.1029/1999JB900353>, 2000.
- Connor, L. J., Connor, C. B., Meliksetian, K., and Savov, I.: Probabilistic approach to modeling lava flow inundation: a lava flow hazard assessment for a nuclear facility in Armenia, *J Appl. Volcanol.*, 1, 3, <https://doi.org/10.1186/2191-5040-1-3>, 2012.
- Danielsen, J. M.: Phreatomagmatic Eruption Deposits on the Seafloor Record Cataclysmic Caldera Formation on Axial Seamount, Juan de Fuca Mid-Ocean Ridge (Doctoral dissertation, San Jose State University)., 2019.
- Deardorff, N. D., Cashman, K. V., and Chadwick, W. W.: Observations of eruptive plume dynamics and pyroclastic deposits from submarine explosive eruptions at NW Rota-1, Mariana arc, *Journal of Volcanology and Geothermal Research*, 202, 47–59, <https://doi.org/10.1016/j.jvolgeores.2011.01.003>, 2011.
- Dietz, R. S. and Sheehy, M. J.: TRANSPACIFIC DETECTION OF MYOJIN VOLCANIC EXPLOSIONS BY UNDERWATER SOUND, *Geol Soc America Bull*, 65, 941, [https://doi.org/10.1130/0016-7606\(1954\)65\[941:TDOMVE\]2.0.CO;2](https://doi.org/10.1130/0016-7606(1954)65[941:TDOMVE]2.0.CO;2), 1954.
- Embley, R., Tamura, Y., Merle, S., Sato, T., Ishizuka, O., Chadwick, W., Wiens, D., Shore, P., and Stern, R.: Eruption of South Sarigan Seamount, Northern Mariana Islands: Insights into Hazards from Submarine Volcanic Eruptions, *oceanog*, 27, 24–31, <https://doi.org/10.5670/oceanog.2014.37>, 2014.
- Gallant, E., Richardson, J., Connor, C., Wetmore, P., and Connor, L.: A new approach to probabilistic lava flow hazard assessments, applied to the Idaho National Laboratory, eastern Snake River Plain, Idaho, USA, *Geology*, 46, 895–898, <https://doi.org/10.1130/G45123.1>, 2018.
- Gregg, T. K. P. and Fornari, D. J.: Long submarine lava flows: Observations and results from numerical modeling, *J. Geophys. Res.*, 103, 27517–27531, <https://doi.org/10.1029/98JB02465>, 1998.
- Harders, R., Ranero, C. R., and Weinrebe, W.: Characterization of Submarine Landslide Complexes Offshore Costa Rica: An Evolutionary Model Related to Seamount Subduction. In S. Krastel et al. (eds.), *Submarine Mass Movements and Their Consequences, Advances in Natural and Technological Hazards Research* 37, DOI 10.1007/978-3-319-00972-8_34, © Springer International Publishing Switzerland 2014, 2014.
- Jutzeler, M., Marsh, R., Carey, R. J., White, J. D. L., Talling, P. J., and Karlstrom, L.: On the fate of pumice rafts formed during the 2012 Havre submarine eruption, *Nat Commun*, 5, 3660, <https://doi.org/10.1038/ncomms4660>, 2014.
- Mel'nikov, M. E., Pletnev, S. P., Anokhin, V. M., Sedysheva, T. E., and Ivanov, V. V.: Volcanic edifices on guyots of the Magellan Seamounts (Pacific Ocean), *Russ. J. of Pac. Geol.*, 10, 435–442, <https://doi.org/10.1134/S1819714016060038>, 2016.
- Moorhouse, B. L., White, J. D. L., and Scott, J. M.: Cape Wanbrow: A stack of Surtseyan-style volcanoes built over millions of years in the Waiareka–Deborah volcanic field, New Zealand, *Journal of Volcanology and Geothermal Research*, 298, 27–46, <https://doi.org/10.1016/j.jvolgeores.2015.03.019>, 2015.
- Murch, A. P., White, J. D. L., and Carey, R. J.: Characteristics and Deposit Stratigraphy of Submarine-Erupted Silicic Ash, Havre Volcano, Kermadec Arc, New Zealand, *Front. Earth Sci.*, 7, 1, <https://doi.org/10.3389/feart.2019.00001>, 2019.

Murtagh, R. M., White, J. D. L., and Sohn, Y. K.: Pyroclast textures of the Ilchulbong 'wet' tuff cone, Jeju Island, South Korea, *Journal of Volcanology and Geothermal Research*, 201, 385–396, <https://doi.org/10.1016/j.jvolgeores.2010.09.009>, 2011.

Németh, K., Cronin, S. J., Charley, D. T., Harrison, M. J., and Garae, E.: Exploding lakes in Vanuatu—"Surtseyan-style" eruptions witnessed on Ambae Island. Massey University. Episodes 29. <http://hdl.handle.net/10179/9629>, 2006.

Newland, E. L., Mingotti, N., and Woods, A. W.: Dynamics of deep-submarine volcanic eruptions, *Sci Rep*, 12, 3276, <https://doi.org/10.1038/s41598-022-07351-9>, 2022.

Ohno, Y., Iguchi, A., Ijima, M., Yasumoto, K., and Suzuki, A.: Coastal ecological impacts from pumice rafts, *Sci Rep*, 12, 11187, <https://doi.org/10.1038/s41598-022-14614-y>, 2022.

Omira, R., Ramalho, I., Terrinha, P., Baptista, M. A., Batista, L., and Zitellini, N.: Deep-water seamounts, a potential source of tsunami generated by landslides? The Hirondele Seamount, NE Atlantic, *Marine Geology*, 379, 267–280, <https://doi.org/10.1016/j.margeo.2016.06.010>, 2016.

Pakoksung, K., Suppasri, A., and Imamura, F.: The near-field tsunami generated by the 15 January 2022 eruption of the Hunga Tonga-Hunga Ha'apai volcano and its impact on Tongatapu, Tonga, *Sci Rep*, 12, 15187, <https://doi.org/10.1038/s41598-022-19486-w>, 2022.

Pansino, S., Emadzadeh, A., and Taisne, B.: Dike Channelization and Solidification: Time Scale Controls on the Geometry and Placement of Magma Migration Pathways, *J. Geophys. Res. Solid Earth*, 124, 9580–9599, <https://doi.org/10.1029/2019JB018191>, 2019.

Paris, R., Switzer, A. D., Belousova, M., Belousov, A., Ontowirjo, B., Whelley, P. L., and Ulvrova, M.: Volcanic tsunamis: a review of source mechanisms, past events and hazards in Southeast Asia (Indonesia, Philippines, Papua New Guinea), *Nat Hazards*, 70, 447–470, <https://doi.org/10.1007/s11069-013-0822-8>, 2014.

Schipper, C. I., White, J. D. L., Zimanowski, B., Büttner, R., Sonder, I., and Schmid, A.: Experimental interaction of magma and "dirty" coolants, *Earth and Planetary Science Letters*, 303, 323–336, <https://doi.org/10.1016/j.epsl.2011.01.010>, 2011.

Scott, J. M., White, J. D. L., and le Roux, P. J.: Intraplate volcanism on the Zealandia Eocene-Early Oligocene continental shelf: the Waiareka-Deborah Volcanic Field, North Otago, New Zealand *Journal of Geology and Geophysics*, 63, 450–468, <https://doi.org/10.1080/00288306.2020.1785896>, 2020.

Sobradelo, R., Geyer, A., and Martí, J.: Statistical data analysis of the CCDB (Collapse Caldera Database): Insights on the formation of caldera systems, *Journal of Volcanology and Geothermal Research*, 198, 241–252, <https://doi.org/10.1016/j.jvolgeores.2010.09.003>, 2010.

Staudigel, H. and Koppers, A. A. P.: Seamounts and Island Building. In: Sigurdsson H, Houghton BF, Rymer H, Stix J, McNutt S (eds) *The encyclopedia of volcanoes*, 2nd edn. Academic Press, New York, pp 405–421, 2015.

Staudigel, H. and Clague, D.: The Geological History of Deep-Sea Volcanoes: Biosphere, Hydrosphere, and Lithosphere Interactions, *Oceanog.*, 23, 58–71, <https://doi.org/10.5670/oceanog.2010.62>, 2010.

Valentine, G. A., White, J. D. L., Ross, P.-S., Graettinger, A. H., and Sonder, I.: Updates to Concepts on Phreatomagmatic Maar-Diatremes and Their Pyroclastic Deposits, *Front. Earth Sci.*, 5, 68, <https://doi.org/10.3389/feart.2017.00068>, 2017.

Verolino, A., White, J. D. L., and Brenna, M.: Eruption dynamics at Pahvant Butte volcano, Utah, western USA: insights from ash-sheet dispersal, grain size, and geochemical data, *Bull Volcanol*, 80, 1–18, <https://doi.org/10.1007/s00445-018-1256-7>, 2018.

Verolino, A., White, J. D. L., Dürig, T., and Cappuccio, F.: Black Point – Pyroclasts of a Surtseyan eruption show no change during edifice growth to the surface from 100 m water depth, *Journal of Volcanology and Geothermal Research*, 384, 85–102, <https://doi.org/10.1016/j.jvolgeores.2019.07.013>, 2019.

Verolino, A., Jenkins, S. F., Sieh, K., Herrin, J. S., Schonwalder-Angel, D., Sihavong, V., and Oh, J. H.: Assessing volcanic hazard and exposure to lava flows at remote volcanic fields: a case study from the Bolaven Volcanic Field, Laos, *J Appl. Volcanol.*, 11, 6, <https://doi.org/10.1186/s13617-022-00116-z>, 2022.

Waters, A. C. and Fisher, R. V.: Base surges and their deposits: Capelinhos and Taal Volcanoes, *J. Geophys. Res.*, 76, 5596–5614, <https://doi.org/10.1029/JB076i023p05596>, 1971.

Wessel, P. and Kroenke, L.: A geometric technique for relocating hotspots and refining absolute plate motions, *Nature*, 387, 365–369, <https://doi.org/10.1038/387365a0>, 1997.